Inorganic Materials, Vol. 40, No. 11, 2004, pp. 1196–1203. Translated from Neorganicheskie Materialy, Vol. 40, No. 11, 2004, pp. 1360–1367.

Mössbauer Study of Tetragonal ZrO_2–Y_2O_3–Fe_2O_3 Solid Solutions

A. G. Belous*, E. V. Pashkova*, A. N. Makarenko*, V. P. Ivanitskii, O. I. V'yunov*, and A. V. Ragulya*****

** Vernadsky Institute of General and Inorganic Chemistry, National Academy of Sciences of Ukraine, pr. Akademika Palladina 32/34, Kiev, 03142 Ukraine*

*** Institute of Geochemistry, Mineralogy, and Ore Formation, National Academy of Sciences of Ukraine, pr. Akademika Palladina 34, Kiev, 03680 Ukraine*

**** Frantsevich Institute of Materials Science Problems, National Academy of Sciences of Ukraine, ul. Krzhizhanovskogo 3, Kiev, 03142 Ukraine*

e-mail: belous@ionc.kar.net

Received November 4, 2003

Abstract—Tetragonal $Zr_{0.886}Y_{0.057}Fe_{0.057}O_{2-\delta}$ solid solutions prepared by calcining coprecipitated and successively precipitated hydroxide mixtures were studied by Mössbauer spectroscopy immediately after calcination and after long-term storage. The results indicate that the solid solutions prepared via coprecipitation and successive precipitation contain Fe^{3+} in two (octahedral coordination) and three (octahedral, fivefold, and tetrahedral coordinations) inequivalent sites, respectively. Partial Fe^{3+} substitution for Y^{3+} is shown to prevent or substantially slow down the low-temperature structural degradation of stabilized zirconia.

INTRODUCTION

The ZrO_2–Y_2O_3–Fe_2O_3 system is of great practical importance in the development of high-strength ceramics [1, 2] and solid electrolytes [3–6]. Partial Fe^{3+} substitution for Y^{3+} in ZrO_2–Y_2O_3 ceramics makes it possible to markedly reduce their sintering temperature [3, 5] and, accordingly, to obtain a fine-grained microstructure, which is essential for achieving high mechanical strength. ZrO_2 and Y_2O_3 are known to form oxygen-deficient substitutional solid solutions (the excess negative charge resulting from Y^{3+} substitution for Zr^{4+} in ZrO_2 is compensated by oxygen vacancies) [7, 8].

There are a number of reports [6, 9, 10] that the ZrO_2–Fe_2O_3 system contains no solid solutions, whereas Teterin *et al.* [11] and Berry *et al.* [12] hold that ZrO_2 dissolves a small amount of Fe_2O_3. According to Neuimin *et al.* [6] and Karavaev *et al.* [10], ZrO_2–Y_2O_3 solid solutions dissolve Fe_2O_3 and Sc_2O_3, and the solubilities of these additives correlate with the content of the stabilizing oxide Y_2O_3. This correlation can be understood in terms of oxygen vacancies (variation in their concentration) in ZrO_2-based solid solutions and the formation of impurity–vacancy defect complexes [10]. The nonlinear temperature variation of the electrical conductivity of ZrO_2-based solid solutions was interpreted by Kotlyar *et al.* [13] as being due to the interaction between oxygen vacancies and solute cations. The interaction between lattice defects and nearest neighbors of stabilizer cations in ZrO_2-based solid solutions was studied in [12–17]. Only a limited number of such studies have been reported for Fe-containing systems [11, 12, 18].

Mössbauer studies of the ZrO_2–Fe_2O_3 system were reported in [11, 12]. According to Teterin *et al.* [11], the products of thermal transformations in this system are α-Fe_2O_3, ZrO_2, Fe^{3+} in a superparamagnetic state, and Fe^{3+} ions dissolved in zirconia. In our opinion, the Mössbauer parameters of the resonance doublets for the Fe^{3+}-containing phases were determined in that study inaccurately, since they were not checked by calibration, and the assignment of the resonance absorption doublets is debatable. The Mössbauer results reported by Berry *et al.* [12] indicate that the Fe-containing cubic ZrO_2 phase formed at 770 and 1020 K at certain Fe concentrations is represented by a quadrupole doublet close in parameters to that of high-spin Fe^{3+} in distorted octahedral coordination. With increasing iron content and calcination temperature, the doublet gives way to a singlet, which may be due to phase transformations or changes in the coordination of Fe^{3+}. Berry *et al.* [12], however, did not specify the parameters of the paramagnetic component, which impedes interpretation of their results.

The lack of data on the defect structure and nature of ZrO_2–Y_2O_3–Fe_2O_3 solid solutions prompted us to undertake a detailed Mössbauer study of this system with the aim of gaining greater insight into the nearest neighbor environment of Fe^{3+} and the interaction between the solute cations and oxygen vacancies. To

rule out the ambiguity associated with the presence of two or three phases in partially stabilized ZrO_2, it is reasonable to investigate stabilized ZrO_2 (single-phase solid solutions). In light of this, we studied single-phase samples of composition $0.94ZrO_2 \cdot 0.03Y_2O_3 \cdot 0.03Fe_2O_3$, which were calcined at 1470 K. The samples were prepared by two procedures and had a tetragonally distorted fluorite structure [19].

Yttria-stabilized ZrO_2 is known to be prone to low-temperature structural degradation because of the tetragonal–monoclinic phase transformation [20]. It is, therefore, also of interest to examine the evolution of the fine structure of the Mössbauer spectrum during long-term storage (aging) of the material.

In this paper, we report a Mössbauer study of the tetragonal solid solution $0.94ZrO_2 \cdot 0.03Y_2O_3 \cdot 0.03Fe_2O_3$ ($Zr_{0.886}Y_{0.057}Fe_{0.057}O_{2-\delta}$) before and after long-term storage, using samples prepared by two procedures.

EXPERIMENTAL

$Zr_{0.886}Y_{0.057}Fe_{0.057}O_{2-\delta}$ samples were prepared by calcining appropriate mixtures of $ZrO(OH)_2$, $Y(OH)_3$, and FeOOH precipitated from concentrated $ZrOCl_2$, $Y(NO_3)_3$, and $Fe(NO_3)_3$ solutions by adding aqueous ammonia. We used two procedures: coprecipitation and successive precipitation. In the latter case, $Y(OH)_3$ was precipitated after $ZrO(OH)_2$ and FeOOH coprecipitation. After washing with distilled water until the wash water was free of Cl^- and NO^{3-}, the precipitates were dried at 350 K and then calcined at 1470 K in a compartment furnace. The samples obtained by successive precipitation were characterized after calcination and after storage under atmospheric conditions for two years.

X-ray diffraction (XRD) measurements were made on a DRON 4-07 powder diffractometer (CoK_α radiation, 40 kV, 18 mA). In phase analysis, we used JCPDS Powder Diffraction File data. Structural parameters were refined by the Rietveld profile analysis method, using the FullProf program. XRD patterns were run in the angular range $2\theta = 10°$–$150°$ in a step-scan mode with a step size $\Delta 2\theta = 0.02°$ and a counting time of 10 s per data point. As external standards, we used SiO_2 (2θ calibration) and Al_2O_3 (intensity standard [21]).

Mössbauer spectra were recorded at room temperature on an electrodynamic spectrometer at a constant acceleration. The gamma source used was ^{57}Co in metallic Rh. In velocity calibration in the magnetic and extended-scale paramagnetic ranges, we used α-Fe and sodium nitroprusside, respectively (the isomer shift relative to α-Fe can be converted to that relative to sodium nitroprusside by adding 0.258 mm/s). In what follows, the isomer shifts in both ranges are specified relative to the respective standard.

Fe content was determined on a Pye Unicom SP 9 atomic absorption spectrophotometer (λ = 248.3 nm, spectral slit width of 0.2 nm, acetylene–air flame). Zr and Y were determined using the fluoride procedure [22]. In addition, Zr was determined as described in [23].

RESULTS AND DISCUSSION

XRD examination showed that the $Zr_{0.886}Y_{0.057}Fe_{0.057}O_{2-\delta}$ samples prepared via both coprecipitation and successive precipitation had a tetragonally distorted fluorite structure (sp. gr. *P*4/*nmc*, no. 137) (Fig. 1, Table 1). In addition, the samples con-

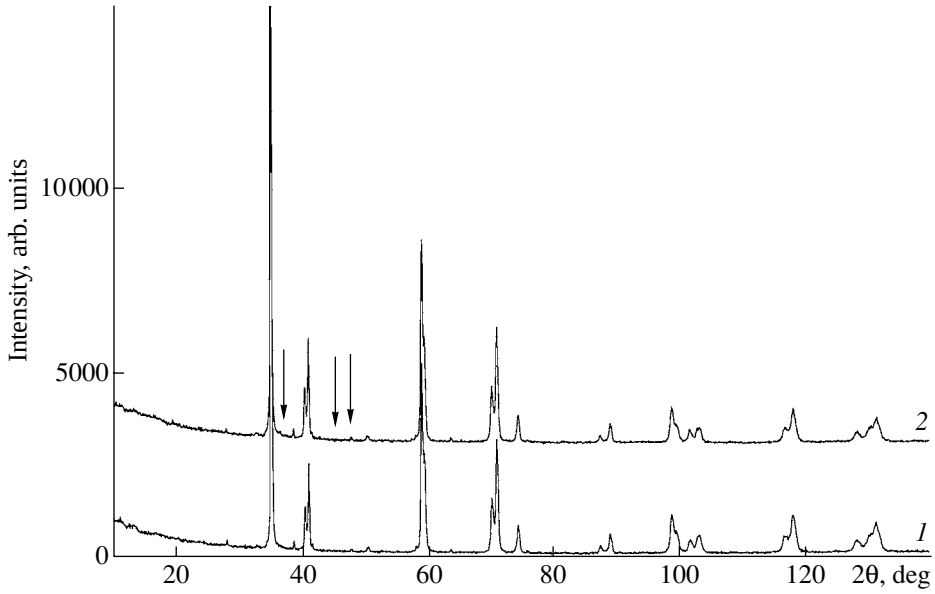

Fig. 1. XRD patterns of $Zr_{0.886}Y_{0.057}Fe_{0.057}O_{2-\delta}$ samples prepared via (*1*) coprecipitation and (*2*) successive precipitation.

Table 1. Structural parameters of $Zr_{0.886}Y_{0.057}Fe_{0.057}O_{2-\delta}$ samples prepared via coprecipitation (CP) and successive precipitation (SP)

Sample	CP	SP
a, Å	3.60562(9)	3.60628(9)
c, Å	5.1693(2)	5.1690(2)
V, Å^3	67.203(3)	67.224(3)
$c/\sqrt{2}a$	1.011(1)	1.013(1)
Thermal parameter B, Å^2		
Zr	0.90(2)	0.08(2)
Y	0.90(2)	0.08(2)
Fe	0.90(2)	0.08(2)
O	2.2(2)	1.6(2)
Site occupancy		
Zr	0.926	0.925
Y	0.058	0.058
Fe	0.016	0.017
O	1.80(2)	1.87(3)
Reliability factors		
R_B, %	2.30	3.19
R_F, %	2.73	2.33
Lattice strain		
η, %	8.7(1)	9.6(1)

Note: Zr–O bond length is 2.218 Å.

tained trace levels of α-Fe_2O_3 (Fig. 1, arrows). Chemical analysis results (Table 2) coincided with the nominal composition to within the present analytical accuracy.

The Mössbauer spectra (magnetic range) of the $Zr_{0.886}Y_{0.057}Fe_{0.057}O_{2-\delta}$ samples prepared via coprecipitation and successive precipitation are shown in Fig. 2, and the parameters of the spectra are listed in Table 3. As seen in Fig. 2, the spectra of the two samples consist of a Zeeman sextet whose parameters agree with those reported for hematite [24, 25] and a quadrupole doublet with parameters characteristic of high-spin Fe^{3+} in octahedral coordination. The sextet due to α-Fe_2O_3 is close in parameters to that arising from bulk, magnetically ordered hematite, which indicates that the solubility of zirconium and yttrium in hematite is insignificant. Such substitutions are typically accompanied by a reduction in H_{eff}. Note that the observed doublets consist of asymmetric absorption lines. The parameters of the doublets differ little from those reported by Berry *et al.* [12], who attributed a similar doublet to Fe^{3+} dissolution in ZrO_2.

The asymmetric shape of the absorption lines and high values of Γ suggest that paramagnetic Fe^{3+} ions are present in at least two phases or in several inequivalent sites, differing in cation and/or anion environments. If the doublets are due to only one phase (tetragonal in this study or cubic in [12]), the asymmetric shape of the absorption lines is attributable to the presence of Fe^{3+} in several inequivalent sites, and the high values of Γ may be associated with a nonuniform cation environment of Fe^{3+}. As shown by Tikhonov and Arsenin [26], lines consisting of several components separated by less than Γ cannot be deconvoluted uniquely. In the case of such spectra, the reliability of deconvolution results can be evaluated from correlation parameters. From the present experimental spectra, we were able to evaluate with certainty the relative amounts of Fe^{3+} in magnetic and paramagnetic phases and to establish that paramagnetic Fe^{3+} ions were present in several inequivalent sites.

To improve the spectral resolution, reduce the experimental error, and elucidate the origin of the

Table 2. Chemical analysis results for $Zr_{0.886}Y_{0.057}Fe_{0.057}O_{2-\delta}$ samples prepared via coprecipitation and successive precipitation

Oxide	Composition, wt %			
	nominal	assay	nominal	assay
	CP		SP	
ZrO_2^*	90.93	91.2	90.93	91.2
ZrO_2^{**}		90.7		90.7
Y_2O_3	5.31	5.3	5.31	5.3
Fe_2O_3	3.76	3.4	3.76	3.4

* Procedure described in [22].

** Procedure described in [23].

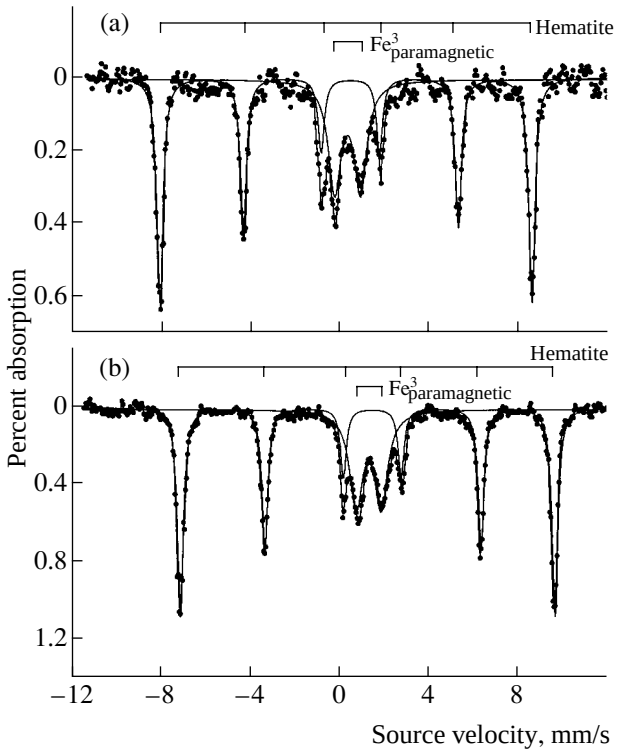

Fig. 2. Mössbauer spectra (magnetic range) of $Zr_{0.886}Y_{0.057}Fe_{0.057}O_{2-\delta}$ samples prepared via (a) coprecipitation and (b) successive precipitation.

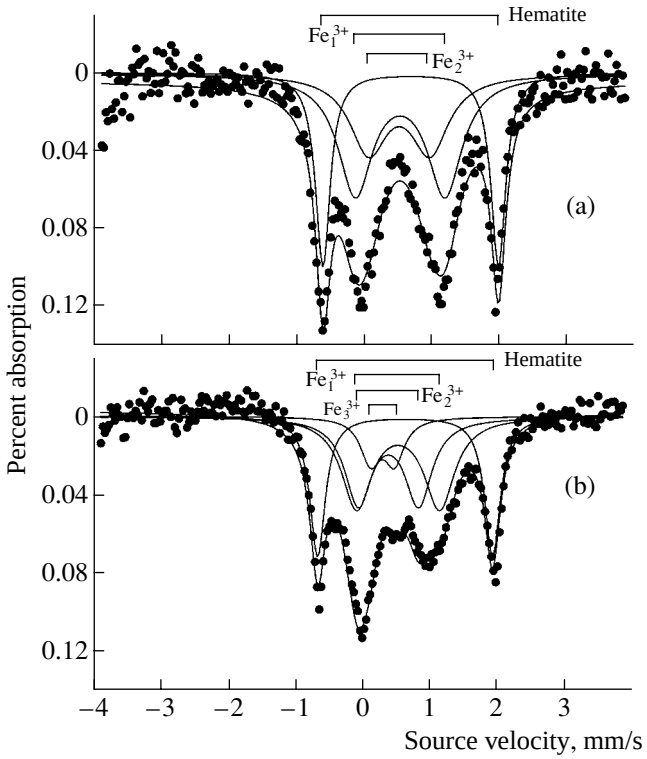

Fig. 3. Mössbauer spectra (paramagnetic range) of $Zr_{0.886}Y_{0.057}Fe_{0.057}O_{2-\delta}$ samples prepared via (a) coprecipitation and (b) successive precipitation.

asymmetry in the shape of the doublet lines, we measured spectra in the paramagnetic range, which offers a resolution more than 3 times as high as that in the magnetic range we used. This allowed us to analyze the structure of the doublets arising from Fe^{3+} in greater detail (Fig. 3). The parameters of the components thus identified are listed in Table 4. The spectra were found to contain two well-resolved lines at –0.56 and 2.05 mm/s, which correspond to the third and fourth lines of the Zeeman sextet due to hematite (Fig. 2). For the convenience of deconvolution and evaluation of the relative contributions of components to the overall spectrum, these two lines were represented by a quadrupole doublet consisting of lines with identical intensities and Γ. The Fe content corresponding to each component was evaluated from its area under the assumptions that the resonance absorption coefficient of Fe^{3+} is the same for all of the coexisting sites and that the intensities of the lines in the sextet due to hematite are in the ratio 3 : 2 : 1 : 1 : 2 : 3. The contribution from the third and fourth lines of the sextet (Fig. 3) is then one-sixth of the total area of the sextet. Multiplying the *S* obtained for the inner lines of hematite by 6 and adding the area of the paramagnetic components, we find the area corresponding to the resonance gamma absorption by all of the Fe^{3+} ions in the sample. The relative con-

Table 3. Mössbauer data (magnetic range) for $Zr_{0.886}Y_{0.057}Fe_{0.057}O_{2-\delta}$ samples

Sample	Ion, phase	H_{eff}, kA/m	IS, mm/s	QS, mm/s	Γ, mm/s	*S*, %
1 (CP)	Hematite	41120	0.38	0.22	0.36	70.3
	$Fe^{3+}_{paramagnetic}$	0	0.33	1.07	0.86	29.7
2 (SP)	Hematite	41200	0.37	0.23	0.32	68.3
	$Fe^{3+}_{paramagnetic}$	0	0.37	1.08	0.90	31.7

Note: H_{eff} = effective magnetic field, IS = isomer shift (relative to α-Fe), QS = quadrupole splitting, Γ = full width at half maximum of the absorption line, *S* = relative area of the component. The measurement accuracy is ±0.04 mm/s in IS, QS, and Γ; ±400 kA/m in H_{eff}; and ≤10% in *S*.

Table 4. Mössbauer data (paramagnetic range) for $Zr_{0.886}Y_{0.057}Fe_{0.057}O_{2-\delta}$ samples

Sample	Ion, phase	IS, mm/s	QS, mm/s	Γ, mm/s	*S*, %	S_0, %
1 (CP)	Hematite	0.76	2.60	0.27	30.5	72.5
	Fe_1^{3+}	0.64	1.33	0.54	42.0	16.6
	Fe_2^{3+}	0.63	0.84	0.53	27.5	10.9
2 (SP)	Hematite	0.75	2.60	0.25	26.6	68.5
	Fe_1^{3+}	0.66	1.21	0.55	36.5	15.7
	Fe_2^{3+}	0.52	0.92	0.46	26.2	11.2
	Fe_3^{3+}	0.43	0.40	0.37	10.7	4.6
2* (SP)	Hematite	0.75	2.61	0.29	29.8	71.8
	Fe_1^{3+}	0.66	1.18	0.52	34.0	13.7
	Fe_2^{3+}	0.49	0.94	0.62	26.4	10.6
	Fe_3^{3+}	0.40	0.44	0.42	9.8	3.9

Note: The same designations as in Table 3. S_0 is the area of the component relative to the sextet of hematite; the isomer shift is given relative to sodium nitroprusside. The measurement accuracy is ±0.03 mm/s in IS, QS, and Γ and ≤10% in *S*.

* Sample 2 after storage under atmospheric conditions for two years.

tribution of each component in the Mössbauer spectrum (S_0, %) can be evaluated using the sum thus obtained (Table 4). Comparison of the data in Tables 3 and 4 demonstrates that, for both samples, the magnetic and paramagnetic contributions related to Fe^{3+} remain unchanged in going from one measurement scale to the other.

The observed features of the inner lines in the spectra in Fig. 3 (asymmetric shape and shoulders) allowed us to identify two doublets (Fe_1^{3+} and Fe_2^{3+}) in the spectrum of the sample prepared by coprecipitation and three doublets in the spectrum of the sample prepared by successive precipitation (Fe_1^{3+}, Fe_2^{3+}, and Fe_3^{3+}).

It follows from the data in Table 4 that the tetragonal zirconia samples studied here dissolve ≈30% of the added Fe^{3+}. The rest of Fe^{3+} (≈70%) is present in the form of α-Fe_2O_3. As shown by Berry *et al.* [12] using electron microscopy, ZrO_2–Fe_2O_3 materials contain regions enriched in one of the constituent cations (clusterlike character of the Zr and Fe distributions. Similar results were reported by Zyuzin *et al.* [18], who revealed structurally disordered clusters 1–1.5 nm in size in $Zr_{0.907}Fe_{0.093}O_{1.953}$ samples prepared by coprecipitation of zirconium and iron hydroxides, followed by calcination at 670 and 970 K. As shown by Chusovitina *et al.* [14] and Voron'ko *et al.* [17], interactions between impurity cations and vacancies in ZrO_2-based solid solutions containing heterovalent substituents may lead to the formation of simple and complex (in terms of composition and structure) associates, or clusters according to West [27]. Such clusters reside, as a rule, in the bulk of ZrO_2 crystallites or, less frequently, in the surface region and lead to the formation of structural defects, such as dislocations, or give rise to bending of lattice planes [27].

The results presented in Fig. 3 and Table 4 lead us to conclude that the $Zr_{0.886}Y_{0.057}Fe_{0.057}O_{2-\delta}$ samples prepared via coprecipitation and successive precipitation contain Fe^{3+} in two and three inequivalent sites, respectively, according to the number of resolved doublets in their spectra. Clearly, inequivalent coordinations of Fe^{3+} may result from different arrangements of vacancies in its nearest neighbor environment and Zr, Y, and Fe cations in its second neighbor environment.

As follows from the data in Table 4, air storage for two years has an insignificant effect on the Mössbauer spectrum of the sample prepared by coprecipitation (samples 2 and 2*), which indicates that, in the ZrO_2–Y_2O_3–Fe_2O_3 system, zirconia experiences very slow or no low-temperature structural degradation, in contrast to the binary system ZrO_2–Y_2O_3 [20].

In interpreting Mössbauer results, QS can be used as a measure of the distortion of coordination polyhedra (deviation from cubic symmetry): changes in the distortion of coordination polyhedra are accompanied by changes in QS. The IS value can be related to the coordination of the Fe^{3+} ion. According to Bencroft *et al.* [28, 29], a decrease

(increase) in the coordination number (CN) of resonance ions is usually accompanied by a decrease (increase) in IS, which is associated with the decrease (increase) in the strength of covalent bonding through 4*s* orbitals upon a decrease (increase) in the cation–oxygen bond length. Eightfold coordination, characteristic of the host cation Zr^{4+} in cubic and tetragonal ZrO_2, is unlikely in the case of Fe^{3+}, not only because of the smaller eightfold-coordinated ionic radius of $Fe^{3+}_{CN=6}$ (0.0645 nm) compared to Zr^{4+} (0.084 nm) [30] but also by virtue of the electroneutrality condition. The negative charge resulting from $2Zr^{4+} \longrightarrow 2Fe^{3+}$ substitution is compensated via the removal of one O^{2-} ion from the anion polyhedron. The reduction in the oxygen–oxygen distance upon partial Fe^{3+} substitution for Y^{3+} ($R_{Y^{3+}_{CN=6}}$ = 0.1015 nm, $R_{Fe^{3+}_{CN=6}}$ = 0.06457 nm [30]) increases the electrostatic repulsion between oxygen ions [31], thereby favoring octahedral coordination of Fe^{3+}.

Given that the high-resolution electron-microscopic studies reported in [12, 18] revealed clustering in ZrO_2–Fe_2O_3 materials, it is reasonable to assume that the presence of several doublets, differing in area, in the Mössbauer spectra of the $Zr_{0.886}Y_{0.057}Fe_{0.057}O_{2-\delta}$ samples (Table 4) is associated with Fe clustering in ZrO_2–Y_2O_3–Fe_2O_3 solid solutions. According to Shpak *et al.* [32], clustering is typical of materials with complex structures and cation or anion substitutions. Clearly, the doublets differing in area (Table 4) correspond to associates (clusters) differing in the number of Fe^{3+} ions and the cation environment of the resonance ions.

Detailed analysis of the present Mössbauer results suggests that the Fe^{3+}_1 and Fe^{3+}_2 doublets in the spectrum of sample 1 and the Fe^{3+}_1, Fe^{3+}_2, and Fe^{3+}_3 doublets in the spectra of samples 2 and 2* are, most likely, due to the presence of Fe^{3+} with CN = 6 (IS = 0.63–0.66 mm/s, QS = 0.84–1.33 mm/s), 5 (IS = 0.49–0.52 mm/s, QS = 0.92–0.94), and 4 (IS = 0.40–0.43, QS = 0.40–0.43), respectively, in the $Zr_{0.886}Y_{0.057}Fe_{0.057}O_{2-\delta}$ solid solution (Table 4).

The cation composition determined with consideration for the Fe content inferred from Mössbauer results (Table 4) was used in refining the oxygen site occupancy by the Rietveld method (Table 1). The actual compositions of the samples prepared via coprecipitation and successive precipitation were determined to be $Zr_{0.926}Y_{0.058}Fe_{0.016}O_{1.80}V_{0.20}$ and $Zr_{0.925}Y_{0.058}Fe_{0.017}O_{1.87}V_{0.13}$, respectively. The higher oxygen content and lattice strain in the latter sample (Table 1) are probably associated with the smaller particle size (larger surface area) of powders prepared by successive precipitation (Fig. 4), which increases oxygen adsorption. This correlates with the results reported by Polezhaev *et al.* [33], who found that air annealing of ZrO_2 or cooling after calcination led to sample oxidation and a reduction in the concentration of oxygen vacancies.

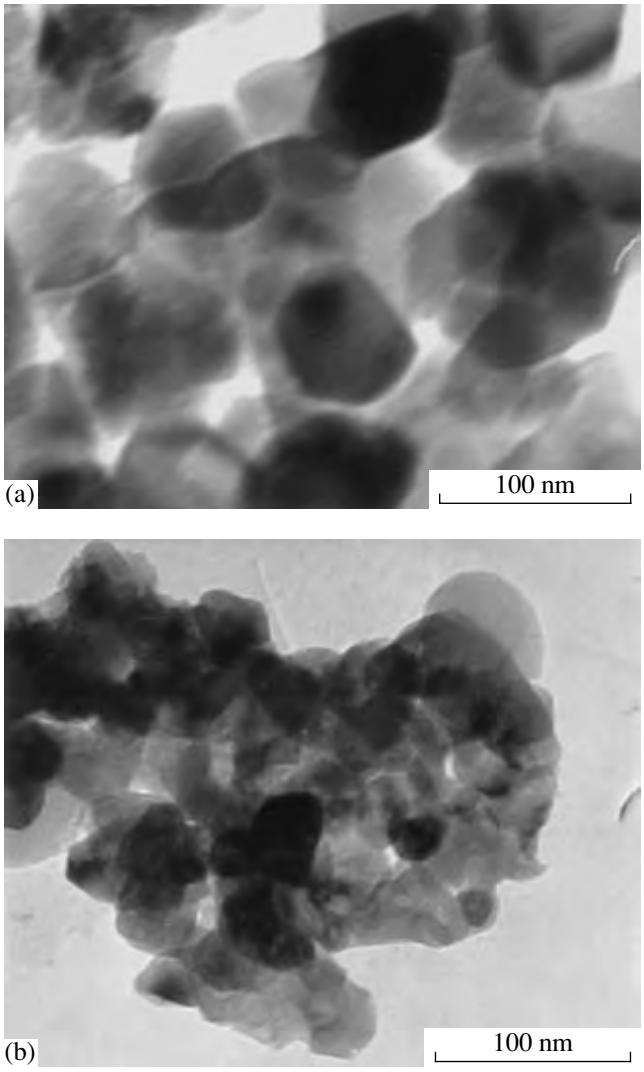

Fig. 4. Electron micrographs of $Zr_{0.886}Y_{0.057}Fe_{0.057}O_{2-\delta}$ samples prepared via (a) coprecipitation and (b) successive precipitation followed by calcination at 1470 K.

CONCLUSIONS

The present Mössbauer results indicate that the tetragonal $Zr_{0.886}Y_{0.057}Fe_{0.057}O_{2-\delta}$ solid solutions prepared by calcining coprecipitated and successively precipitated hydroxide mixtures contain Fe^{3+} in two (octahedral coordination) and three (octahedral, fivefold, and tetrahedral coordinations) inequivalent sites, respectively. Partial Fe^{3+} substitution for Y^{3+} is shown to stabilize tetragonal ZrO_2–Y_2O_3 solid solutions.

As shown by the Rietveld profile analysis method, the oxygen content (concentration of oxygen vacan-

cies) in the samples depends on the preparation procedure.

REFERENCES

1. Dedov, N.V., Konasov, V.A., Matyukha, V.A., and Solov'ev, A.I., Plasma Synthesis and Properties of Zirconia-Based Ceramics, *Ul'tradispersnye poroshki, materialy i nanostruktury; poluchenie, svoistva, primenenie: Materialy mezhregional'noi konferentsii s mezhdunarodnym uchastiem* (Proc. Int. Conf. on the Preparation, Properties, and Applications of Ultrafine Powders and Materials and Nanostructures), Krasnoyarsk, 1996, pp. 126–127.
2. Gogotsi, G.A., Galenko, V.I., and Ozerskii, B.I., Fracture Toughness and Other Properties of Partially Stabilized Zirconia Ceramics with Iron Oxide Additions, *Ogneupory Tekh. Keram.*, 1996, no. 2, pp. 2–8.
3. Karavaev, Yu.I. and Burmakin, E.I., Effect of Ferric Oxide on the Conductivity of Yttria-Stabilized Tetragonal Zirconia Solid Electrolytes, *Neorg. Mater.*, 1996, vol. 32, no. 1, pp. 66–70 [*Inorg. Mater.* (Engl. Transl.), vol. 32, no. 1, pp. 58–61].
4. Matsui, N. and Takigawa, H., Impedance on YSZ with Iron Oxide as Additive, *Solid State Ionics*, 1990, vol. 40, no. 41, pp. 926–928.
5. Karavaev, Yu.I., Martem'yanova, Z.S., and Zyryanov, V.G., Effect of Ferric Oxide on the Structure of Solid Solutions in the ZrO_2–Y_2O_3–Fe_2O_3 System, *Neorg. Mater.*, 1995, vol. 31, no. 7, pp. 937–941 [*Inorg. Mater.* (Engl. Transl.), vol. 31, no. 7, pp. 861–866].
6. Neuimin, A.D., Kotlyar, A.G., Pal'guev, S.F., *et al.*, Structure and Electrical Conductivity of Y_2O_3-Stabilized ZrO_2 with Additions of Iron, Manganese, Cobalt, and Nickel Oxides, *Tr. Inst. Elektrokhim., Ural. Fil., Akad. Nauk SSSR*, 1969, no. 12, pp. 92–95.
7. Strekalovskii, V.N., Polezhaev, Yu.M., and Pal'guev, S.F., *Oksidy s primesnoi razuporyadochennost'yu* (Oxides with Impurity Disordering), Moscow: Nauka, 1987.
8. Chebotin, V.N. and Perfil'ev, M.V., *Elektrokhimiya tverdykh elektrolitov* (Electrochemistry of Solid Electrolytes), Moscow: Khimiya, 1978.
9. Escribe, C. and Van der Voort, E., Energy Calculations of Generated by Dissolution of Cd and Fe in Monoclinic Zirconia, *Phys. Status Solidi A*, 1976, vol. 36, no. 1, pp. 375–378.
10. Karavaev, Yu.N., Neuimin, A.D., and Pal'guev, S.F., Effects of Iron, Chromium, Titanium, and Rare-Earth Oxides on the Formation of Cubic Solid Solutions in the System ZrO_2–Sc_2O_3, *Izv. Akad. Nauk SSSR, Neorg. Mater.*, 1985, vol. 21, no. 7, pp. 1172–1175.
11. Teterin, G.A., Menchuk, E.M., Egorov, F.K., *et al.*, Reaction Kinetics in the Systems TiO_2–Fe_2O_3 and ZrO_2–Fe_2O_3, *Ukr. Khim. Zh.* (Russ. Ed.), 1986, vol. 52, no. 7, pp. 696–700.
12. Berry, F.J., Loretto, M.H., and Smith, M.R., Iron–Zirconium Oxides: An Investigation of Structural Transformation by X-ray Diffraction, Electron Diffraction, and Iron-57 Mossbauer Spectroscopy, *J. Solid State Chem.*, 1989, vol. 83, no. 1, pp. 91–99.
13. Kotlyar, A.G., Neuimin, A.G., Pal'guev, S.F., *et al.*, Electrochemistry of Molten Salts and Solid Electrolytes, *Tr. Inst. Elektrokhim., Ural. Fil., Akad. Nauk SSSR*, 1970, no. 16.
14. Chusovitina, T.V., Toropov, Yu.S., Rutman, D.S., and Pliner, S.Yu., Defect Interactions in $0.90ZrO_2 \cdot 0.10M_2O_3$ Solid Solutions, *Izv. Akad. Nauk SSSR, Neorg. Mater.*, 1986, vol. 22, no. 6, pp. 969–973.
15. Hashimoto Shinya, Iwasaki Hiroshi, Ogawa Shiro, *et al.*, A New Type of Ordered Arrangement of Interstitial Oxygen Atoms in the Solid Solution of the Zr–O System, *J. Phys. Soc. Jpn.*, 1972, vol. 32, no. 4, p. 1146.
16. Strekalovskii, V.N., Makurin, Yu.N., Kasimov, G.G., and Vovkotrub, E.G., Dehydration and Defect Formation during the Preparation of Fluorite-Structure Oxides, *Izv. Akad. Nauk SSSR, Neorg. Mater.*, 1986, vol. 22, no. 3, pp. 2067–2070.
17. Voron'ko, Yu.K., Zufarov, M.A., Sobol', A.A., and Tsymbal, L.I., Site-Selective Spectroscopy and Nearest Neighbor Environment of Eu^{3+} in Monoclinic ZrO_2–Ln_2O_3 and HfO_2–Ln_2O_3 Solid Solutions, *Neorg. Mater.*, 1996, vol. 32, no. 10, pp. 1213–1219 [*Inorg. Mater.* (Engl. Transl.), vol. 32, no. 10, pp. 1063–1068].
18. Zyuzin, D.A., Moroz, E.M., Ivanova, A.S., and Zaikovskii, V.I., Structural Study of X-ray Amorphous Fe–Zr–O Materials, *Neorg. Mater.*, 2000, vol. 36, no. 4, pp. 447–451 [*Inorg. Mater.* (Engl. Transl.), vol. 36, no. 4, pp. 359–363].
19. Belous, A.G., Pashkova, E.V., Makarenko, A.N., *et al.*, Phase Composition of Heat-Treatment Products in the $ZrO(OH)_2$–$Y(OH)_3$–FeOOH System, *Neorg. Mater.*, 2001, vol. 37, no. 3, pp. 314–319 [*Inorg. Mater.* (Engl. Transl.), vol. 37, no. 3, pp. 248–253].
20. Wang, J. and Stevens, R., Preferred ZrO_2(t)–ZrO_2(m) Transformation on the Aged Surface of TZP Ceramics, *J. Mater. Sci. Lett.*, 1989, vol. 8, no. 10, pp. 1195–1198.
21. *Certificate of Analysis: Standard Reference Material 1976, Instrument Sensitivity Standard for X-ray Powder Diffraction*, Gaithersburg: National Inst. of Standards and Technology, 1991, pp. 1–4.
22. Knipovich, Yu.N. and Marachevskii, Yu.V., *Analiz mineral'nogo syr'ya* (Analysis of Mineral Raw Materials), Leningrad: Khimizdat, 1956, 2nd ed.
23. *GOST* (State Standard) *10398-76: Reagents; Chelatometric Determination of the Major Substance*, 1976.
24. Kistner, O.C. and Sunyar, A.W., Evidence for Quadrupole Interaction of Fe^{57m} and Influence of Chemical Binding on Nuclear Gamma-Ray Energy, *Phys. Rev. Lett.*, 1960, vol. 4, no. 8, pp. 412–415.
25. Shirane, G., Cox, D.E., and Ruby, S.L., Mossbauer Study of Isomer Shift, Quadrupole Interaction, and Hyperfine Field in Several Oxides Containing Fe^{57}, *Phys. Rev.*, 1962, vol. 125, no. 4, pp. 1158–1165.
26. Tikhonov, A.N. and Arsenin, V.Ya., *Metody resheniya nekorrektnykh zadach* (Solutions of Ill-Posed Problems), Moscow: Nauka, 1979, 2nd ed.

27. West, A.R., *Solid State Chemistry and Its Applications*, Chichester: Wiley, 1984. Translated under the title *Khimiya tverdogo tela*, Moscow: Mir, 1988, pp. 440–441.

28. Bencroft, G., Maddock, A., and Barnes, R., Mössbauer Effect Applications in Silicate Mineralogy: I. Iron Silicates with Known Structures, in *Fizika mineralov* (Physics of Minerals), Moscow: Mir, 1971, pp. 179–204.

29. Bencroft, G., Barnes, R., and Stone, A., Mössbauer Effect Applications in Silicate Mineralogy: II. Iron Silicates with Unknown and Complex Crystal Structures, in *Fizika mineralov* (Physics of Minerals), Moscow: Mir, 1971, pp. 205–216.

30. Shannon, R.D. and Prewitt, C.T., Effective Ionic Radii in Oxides and Fluorides, *Acta Crystallogr., Sect. B: Struct. Crystallogr. Cryst. Chem.*, 1969, vol. 25, no. 5, pp. 925–946.

31. Ol'khovik, G.A., Naumov, I.I., Velikokhatnyi, O.I., and Aparov, N.N., Electronic Structure and Optical Properties of ZrO_2 Doped with Yttrium, *Neorg. Mater.*, 1993, vol. 29, no. 5, pp. 636–640 [*Inorg. Mater.* (Engl. Transl.), vol. 29, no. 5, pp. 545–549].

32. Shpak, A.P., Kunitskii, Yu.A., and Samoilenko, Z.A., *Samoorganizatsiya struktury v materialakh razlichnoi prirody* (Structural Self-organization in Various Materials), Kiev: Akademkniga, 2002.

33. Polezhaev, Yu.M., Mikshevich, M.V., Pilipenko, G.I., and Lakhov, V.M., Formation and Annealing of Anion Defects during Thermal Decomposition of Zirconium Hydroxide in Vacuum, *Izv. Akad. Nauk SSSR, Neorg. Mater.*, 1976, vol. 12, no. 6, pp. 1052–1056.